Available online at www.sciencedirect.com
SCIENCE DIRECT®
Journal of Catalysis 228 (2004) 56–65
JOURNAL OF CATALYSIS
www.elsevier.com/locate/jcat

# Production of hydrogen from oxidative steam reforming of methanol II. Catalytic activity and reaction mechanism on $Cu/ZnO/Al_2O_3$ hydrotalcite-derived catalysts

M. Turco [a,*], G. Bagnasco [a], U. Costantino [b], F. Marmottini [b], T. Montanari [c], G. Ramis [c], G. Busca [c]

[a] *Dipartimento di Ingegneria Chimica, Università di Napoli Federico II, P.le V. Tecchio 80, 80125 Napoli, Italy*
[b] *CEMIN – Centro Eccellenza Materiali Innovativi Nanostrutturati, Dipartimento di Chimica, Università di Perugia, Via Elce di Sotto 8, 06123 Perugia, Italy*
[c] *Dipartimento di Ingegneria Chimica e di Processo "G.B. Bonino", Università di Genova, P.le J.F. Kennedy 1, 16129 Genova, Italy*

Received 10 May 2004; revised 30 July 2004; accepted 17 August 2004

Available online 25 September 2004

**Abstract**

$Cu/ZnO/Al_2O_3$ catalysts derived from a hydrotalcite precursor were studied for oxidative steam reforming of methanol (OSRM), with $O_2$:$H_2O$:$CH_3OH$ molar ratios = 0.12:1.1:1. The results were compared with those obtained in nonoxidative steam reforming (SRM) and in partial oxidation (POM) of methanol. The catalysts were highly active for OSRM, giving total $CH_3OH$ conversion at 350–400 °C with GHSV = 0.6–1.2 × $10^5$ $h^{-1}$. They also showed high selectivity, giving $H_2$ yield of 2.5 mol per mole $CH_3OH$, with CO concentration below 500 ppm. Besides the main products, $CH_2O$ and $(CH_3)_2O$ were also observed at all temperatures, while some $CH_4$ was produced at $T > 300$ °C. The catalytic activity increased with increasing heating rate of the catalyst precursor. High selectivity was observed also in SRM, but with lower conversion. On the other hand, POM appeared faster than SRM, but produced CO concentrations of a few percent at $T > 300$ °C, due to $CH_3OH$ decomposition. The production of CO was strongly reduced in the presence of water vapor. The reaction network was described in detail. The interaction methanol catalyst was studied by IR spectroscopy. IR spectra showed the presence of adsorbed methoxy groups, that were converted into formate groups at high temperature, and then decomposed into $H_2$ and CO in the absence of $O_2$ and/or $H_2O$, while in their presence CO was probably oxidized to $CO_2$ before desorption, due to the action of Cu(II) species.


*Keywords:* Methanol steam reforming; Methanol partial oxidation; Hydrogen production; $Cu/ZnO/Al_2O_3$ catalysts; Hydrotalcite; Methanol adsorption; Reaction mechanism; Reaction network

## 1. Introduction

Methanol appears to be a suitable liquid source for on-board production of hydrogen in the case of fuel cell electric engine cars and boats. A suitable process should produce $H_2$ in high concentration to obtain high performances of the fuel cells [1]. Additionally CO impurity in $H_2$ must be very low (< 20 ppm) because it poisons the platinum anodes of fuel cells [2–4].

Hydrogen can be produced from methanol by different reactions. The most simple reaction is endothermic decomposition that allows the production of 1:2 mol/mol CO and $H_2$ mixtures: these must be further treated with water to convert CO to $CO_2$ through the water gas shift reaction (WGS).

$$CH_3OH(g) = CO + 2H_2, \quad \Delta H^0 = 90.6 \text{ kJ mol}^{-1}, \tag{1}$$

$$CO + H_2O(g) = CO_2 + H_2, \quad \Delta H^0 = -41.1 \text{ kJ mol}^{-1}. \tag{2}$$

The second exothermic step can be performed at low temperatures in order to limit the CO content in the gas; however, this reaction does not allow reduction of the CO content

* Corresponding author. Fax: +39 081 5936936.
*E-mail address:* turco@unina.it (M. Turco).

0021-9517/$ – see front matter 
doi:10.1016/j.jcat.2004.08.029

below 5000 ppm [5]. The two reactions (1) + (2) can be obtained in one step with the socalled methanol catalytic steam reforming (SRM), according to [3,6–15]

$$CH_3OH(g) + H_2O(g) = CO_2 + 3H_2, \quad \Delta H^0 = 49.5\ \text{kJ mol}^{-1}. \tag{3}$$

This process allows high hydrogen yield and high concentration of $H_2$ in the gaseous mixture (up to 75%). However, since the reaction is endothermic, the reformer needs to be heated, and this leads to some drawbacks, such as starting delay and difficulty in obtaining rapid variations of speed [3]. Also, due to the relatively high temperature needed, residual CO cannot be pushed very low because of the equilibrium (2).

Another widely studied reaction for $H_2$ production is methanol partial oxidation (POM), according to [16–22]

$$CH_3OH(g) + \frac{1}{2}O_2 = CO_2 + 2H_2, \quad \Delta H^0 = -192.3\ \text{kJ mol}^{-1}. \tag{4}$$

The POM process has the advantages of being fast and suitable for rapid speed variations. However this process, compared to SRM, leads to a lower yield to $H_2$ and to lower $H_2$ concentration. The maximum theoretical $H_2$ concentration is 67%, but since the use of pure oxygen is not technically feasible for car traction, air must be used as oxidant, so the maximum hydrogen concentration is 41%. Other drawbacks are related to the exothermicity of the reaction: high release of heat decreases power efficiency, temperature control of the reactor is difficult, and hot spots can occur in the catalyst, leading to reduction of activity [23]. On the other hand, with this process residual CO could be reduced to trace amounts if the catalyst were highly active for the $CO + O_2$ reaction. In practice, both SRM and POM produce appreciable CO amounts, strongly depending on the nature of the catalyst and operating conditions [7,24].

Recently a new process based on combination of SRM and POM reactions, named oxidative steam reforming of methanol (OSRM) has been proposed [1,23–30]. By feeding $CH_3OH$, $H_2O$, and $O_2$ (air) in proper amounts, the heat released by POM balances that taken up by SRM and required for heating the reactants. In this way, an autothermal process is obtained, thus leading to a more easily controlled system. This allows delivery of high hydrogen concentration gas (up to 65%, if air is used) [23] and can be suited for rapid startup and power variations by properly varying the methanol/oxygen ratio [1]. Moreover, under proper conditions, OSRM can produce hydrogen containing very low CO concentrations [24,26,27].

As described in the first part, the OSRM catalysts proposed in the literature are mostly based on copper dispersed on metal oxides such as $Al_2O_3$ or $ZrO_2$, often with the presence of ZnO that acts as a promoter [29,31]. Systems derived from mixed hydroxycarbonates with hydrotalcite structure appear very promising for high $H_2$ yield and low CO production [26,27].

Some aspects of the OSRM process need further investigation. The reaction network of OSRM is very complex and not yet defined. In the reacting system, besides SRM and POM, other reactions, such as combustion and decomposition of methanol, can also occur [8,24,27,28]. The pathway of CO formation is widely debated [8,22,27,32,33]. Moreover different points of view are reported regarding the nature of the active sites and reaction mechanisms [6,7,34,35].

In Part I of this paper the preparation and wide characterization of Cu/Zn/Al hydrotalcite-like precursor, obtained by the method of homogeneous precipitation induced by urea hydrolysis, and of the derived catalysts have been reported [31]. In this paper we will describe the catalytic activity of the materials obtained and the effects of operating conditions. Reaction paths and mechanistic studies based on IR experiments will also be described and discussed.

## 2. Experimental

The catalyst precursor was prepared via precipitation of Zn, Cu, and Al chlorides in the presence of urea, according to the previously described method [31]. The precipitate consisting of Cu/Zn/Al hydrotalcite and Zn/Cu paratacamite, in the mass weight ratio of 3 to 1, was heated in dry air flow at rate of 2 or 10 °C $\text{min}^{-1}$ up to 450 °C and maintained at this temperature for 12 h. Then the samples were reduced in situ in 2% $H_2$/He mixture at 450 °C for 2 h. The two catalysts, consisting mainly of Cu, Zn, and Al oxides, were named 2-Cu/Zn/Al and 10-Cu/Zn/Al, respectively, according to the heating rate of the precursor. Catalytic activity measurements were carried out in a laboratory flow apparatus with a fixed-bed reactor operating at atmospheric pressure. The catalyst (size = 90–110 μm) was diluted with fused-quartz powders in 1:10 ratio to obtain isothermal conditions. The reactor was equipped with two lines for liquid and gaseous feeding. Liquid feed ($H_2O/CH_3OH$) was introduced by metering pumps and gaseous feed ($O_2$, He) by electronic flow controllers. A gas chromatograph HP 5890 equipped with a Porapak/molecular sieve double-packed column and a TCD detector allowed analysis of $H_2$, CO (detection limit = 0.05%), $CO_2$, $O_2$, $CH_4$, $CH_3OH$, and $H_2O$. From the concentrations and flow rates of the effluent stream, total and partial conversions were calculated. A Hiden mass spectrometer was also employed for identification of products not detected by GC. The used catalyst samples were analyzed for organic compounds by an LECO Corporation CHN 2000 elemental analyzer. The OSRM tests were carried out with catalyst mass of 0.045 or 0.09 g (apparent density = 1 g $\text{cm}^{-3}$), at $T$ = 200–400 °C, $H_2O/CH_3OH/O_2$ molar ratios = 1.1/1/0.12 ($CH_3OH$ concentration = 17.8%), GHSV = $0.6 \times 10^5$, $1.2 \times 10^5$ $\text{h}^{-1}$. SRM and POM tests were carried out under the same conditions, but without feeding $O_2$ or $H_2O$, respectively; methanol decomposition (DEC) was tested excluding both $H_2O$ and $O_2$. Each test lasted 1.5–2 h and in

this time the products were sampled and analyzed two or three times: it was verified that conversion values were constant. It was ascertained in preliminary tests that diffusive resistances were negligible.

The IR spectra were recorded with a Nicolet Protégé 460 Fourier transform instrument. A conventional manipulation/outgassing ramp connected to the IR cell was used. Pressed disks of pure catalyst powder (15 mg, 2 cm diameter) were used. The sample was thermally pretreated by outgassing at 450 °C in the IR cell. The adsorption procedure involves contact of the activated sample disk with the methanol vapor at 250 °C in situ and outgassing in steps from 250 °C to higher temperatures. In order to better evaluate the surface species from all the spectra herein reported the spectrum of the pretreated catalyst has been subtracted.

## 3. Results and discussion

### 3.1. Catalytic activity measurements

In preliminary tests it was ascertained that no reactions occurred in the absence of catalysts under all the experimental conditions investigated.

In OSRM tests the reaction products analyzed by GC are $H_2$, $CO_2$, $O_2$, $CH_4$, $CH_3OH$, and $H_2O$. Carbon monoxide was in a concentration below the detection limit of our apparatus (0.05%). In addition, MS analysis identified $CH_2O$ and $(CH_3)_2O$, while $HCOOCH_3$, alkenes, and higher alkanes were not detected. Taking into account that $CH_2O$ and $(CH_3)_2O$ are not quantitatively analyzed by our GC, the total amount $CH_2O + (CH_3)_2O$ is evaluated from a mass balance. Elemental analysis of carbon, carried out on the used catalysts, ascertained that no carbon compounds were present.

The results of OSRM tests on 2-Cu/Zn/Al are reported in Figs. 1 and 2. Catalytic activity is markedly influenced by temperature and space velocity. At GHSV $= 1.2 \times 10^5\ h^{-1}$ (Fig. 1a) $CH_3OH$ conversion appears negligible at $T <$ 300 °C but it increases rapidly with temperature, reaching 90% at 400 °C. $H_2$ yield, defined as $H_2$ moles per $CH_3OH$ moles, is negligible at low temperatures and reaches a value of about 2 at 400 °C. Conversions of methanol to different products are reported in Fig. 1b, where $C_xH_yO$ means the total amount $(CH_3)_2O + CH_2O$. At low temperatures conversion to $CO_2$ is negligible while some conversion to $C_xH_yO$ is observed, suggesting that methanol dehydration and/or dehydrogenation is prevailing under these conditions. No other products are observed up to 300 °C. By increasing temperature, conversion to $CO_2$ markedly increases up to 80% at 400 °C while conversion to $C_xH_yO$ reaches a maximum at 350 °C and sharply decreases at 400 °C. $CH_4$ is formed in an appreciable amount (5%) only at 400 °C. CO is less than the detection limit (0.05%) at all temperatures. At GHSV $= 0.6 \times 10^5\ h^{-1}$ (Fig. 2a) $CH_3OH$ conversion shows a similar trend but with higher values in comparison to GHSV $= 1.2 \times 10^5\ h^{-1}$, being appreciable even from

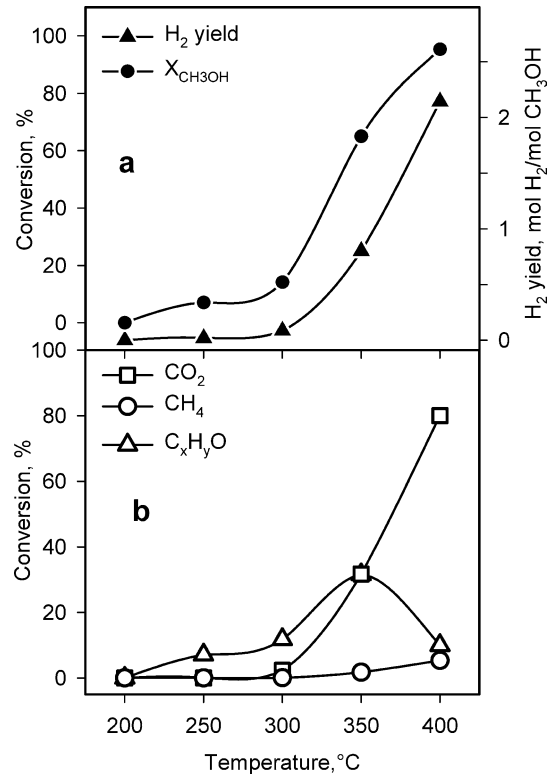


Fig. 1. (a) Methanol conversion and hydrogen yield; (b) conversions to different products as a function of temperature under OSRM conditions for the catalyst 2-Cu/Zn/Al, GHSV $= 1.2 \times 10^5\ h^{-1}$.

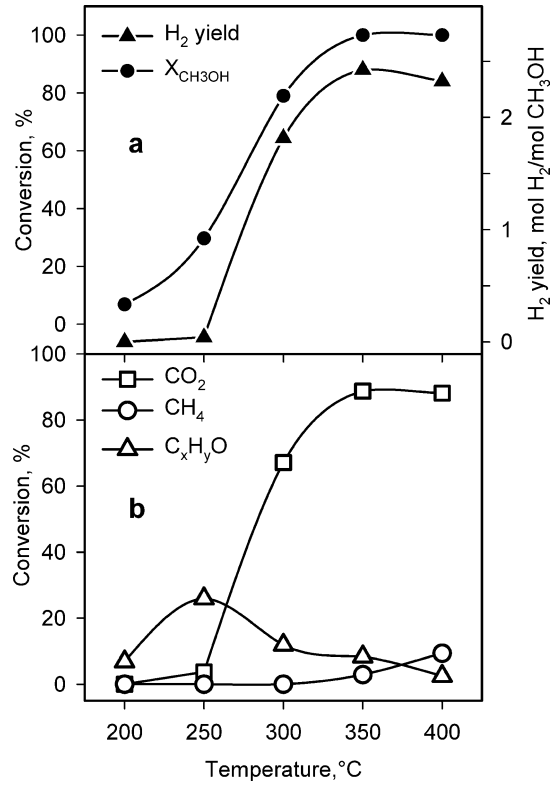


Fig. 2. (a) Methanol conversion and hydrogen yield; (b) conversions to different products as a function of temperature under OSRM conditions for the catalyst 2-Cu/Zn/Al, GHSV $= 0.6 \times 10^5\ h^{-1}$.

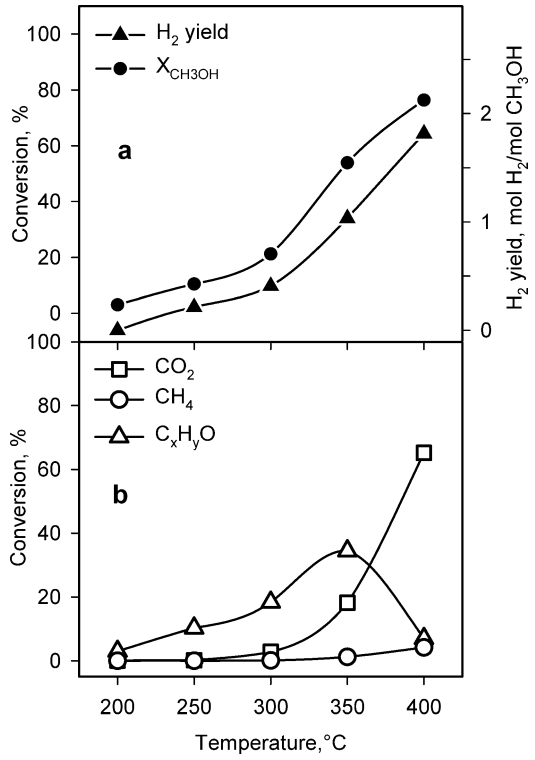


Fig. 3. (a) Methanol conversion and hydrogen yield; (b) conversions to different products as a function of temperature under OSRM conditions for the catalyst 10-Cu/Zn/Al, GHSV = $1.2 \times 10^5$ $h^{-1}$.

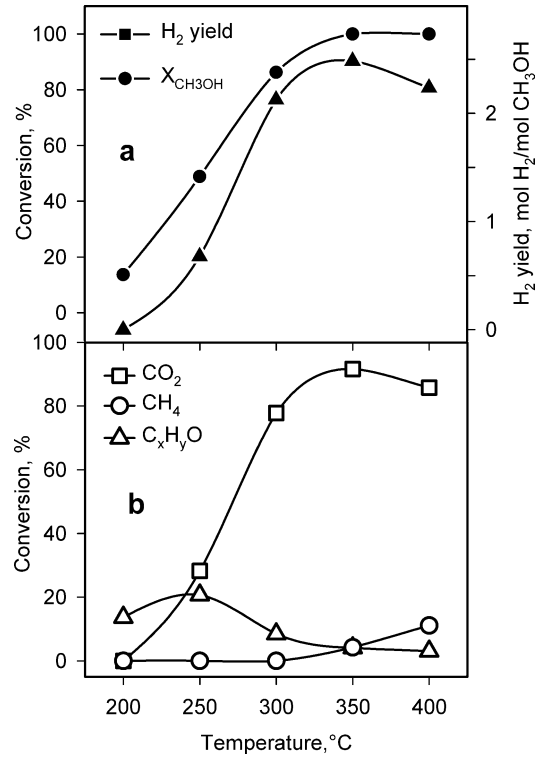


Fig. 4. (a) Methanol conversion and hydrogen yield; (b) conversions to different products as a function of temperature under OSRM conditions for the catalyst 10-Cu/Zn/Al, GHSV = $0.6 \times 10^5$ $h^{-1}$.

200 °C and complete at 350 °C. At the same time $H_2$ yield, that was negligible up to 300 °C with the higher GHSV, gives a value of about 2 at 300 °C, and at 350 °C reaches a value of 2.5: this is close to the theoretical value (2.8) assuming a total conversion of $CH_3OH$ and $O_2$. Conversion to $CO_2$ (Fig. 2b) parallels $H_2$ yield, since it is very low at $T < 300$ °C and sharply increases with temperature up to about 90% at 350–400 °C. $C_xH_yO$ are prevailing at low temperatures, showing a maximum at 250 °C. It is remarkable that the formation of these compounds increases by decreasing GHSV at low temperatures, while the opposite behavior is observed at high temperatures: this results into shifting of the maximum of the $C_xH_yO$ conversion curve to lower temperatures with the lower GHSV. $CH_4$ conversion is appreciable only at high temperatures and reaches a value of about 9% at 400 °C, which is higher than that observed at GHSV = $1.2 \times 10^5$ $h^{-1}$. The CO concentration is below the detection limit also in the tests carried out at GHSV = $0.6 \times 10^5$ $h^{-1}$.

The results of the OSRM tests on 10-Cu/Zn/Al are reported in Figs. 3 and 4. The reaction products are the same as those observed for 2-Cu/Zn/Al. Methanol conversions, hydrogen yield, and partial conversions are comparable to those of 2-Cu/Zn/Al and appear similarly influenced by temperature and space velocity. However, it can be noted that the 10-Cu/Zn/Al sample is more active at low temperatures, as shown by the higher values of $CH_3OH$ conversion and $H_2$ yield: methanol conversion reaches about 50% with $H_2$ yield of 0.7 at 250 °C. It is worth noting that at 200 °C and GHSV = $0.6 \times 10^5$ $h^{-1}$ 15% methanol conversion is observed, without any $H_2$ production, $C_xH_yO$ being the only reaction products, suggesting that at low temperatures only dehydration and dehydrogenation occur. A similar behavior is exhibited by 2-Cu/Zn/Al, but to a lower extent.

These results show that the behavior of the two samples is not substantially different, although the sample 10-Cu/Zn/Al appears more active at low temperatures. This could be related to different redox properties, as shown by TPR and TPO measurements [31]. In fact the sample 10-Cu/Zn/Al has a larger fraction of Cu species that undergo reduction and oxidation at low temperatures and can be catalytically active. This is probably related to the higher Cu dispersion of this catalyst [31]. The correlation between the Cu reduction temperature and the catalytic activity was reported by other authors [29]. Another effect could be taken into account to explain the different activity at low temperatures. The samples 2-Cu/Zn/Al and 10-Cu/Zn/Al have markedly different surface areas, 73 and 111 $m^2$ $g^{-1}$, respectively [31]. The higher surface area, which is probably due mainly to amorphous alumina, corresponds to a higher amount of surface acid sites: this condition could lead to higher activity for dehydration, thus explaining the higher activity at 200 °C. The activity of the present catalysts, evaluated as $H_2$ yield and CO production, can be compared with literature data on similar systems. Velu et al. [34] studied a Cu/Zn/Al catalyst (at. ratio = 37/51/12) derived from hydrotalcite–

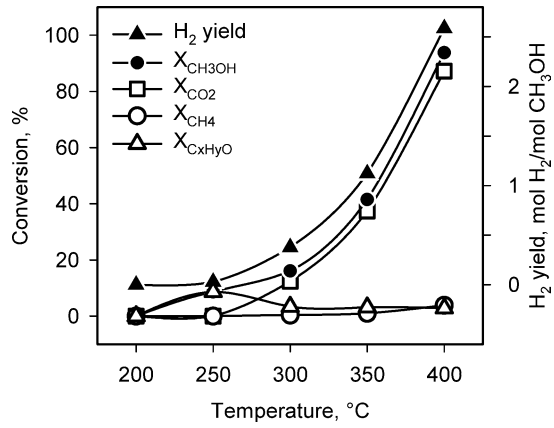


Fig. 5. Methanol conversion, hydrogen yield, and conversions to different products as a function of temperature under SRM conditions for the catalyst 10-Cu/Zn/Al, GHSV $= 0.6 \times 10^5\ h^{-1}$.

aurichalcite phases and tested under similar operating conditions and found methanol conversion of about 60–65%, with $H_2$ yield of about 2 mol $mol^{-1}$ in the temperature range 200–260 °C. The CO concentration in the product stream was 300–1200 ppm. With a catalyst of similar composition but under somewhat different conditions Agrell et al. [24] report $CH_3OH$ conversions of 50–90% and CO concentrations of 300–1300 ppm at temperatures of 270–325 °C. Murcia-Mascarós et al. [26] report data for a hydrotalcite-derived Cu/Zn/Al catalyst with compositions more similar to the present system (at. ratio = 22/37/41), tested under similar conditions, obtaining methanol conversions of about 50–70% and $H_2$ yield of 1.6 mol $mol^{-1}$ at 270–325 °C: the CO content in the effluent stream was 1500–4000 ppm. Shen and Song [29] studied a coprecipitated Cu/Zn/Al catalyst (at. ratio = 45/43/12) with a similar feed composition, but much lower GHSV than ours (~22,000 $h^{-1}$) obtaining conversion of 99% at 230 °C and CO concentration of about 500 ppm. Also supported systems were studied: alumina supported Cu/Zn catalysts [23] gave high methanol conversion (up to 90% at 300 °C) and $H_2$ yield (up to 2.8) with GHSV = 25,000 $h^{-1}$, however, with higher CO concentrations (1.1%). On the basis of these results, taking into account differences in catalyst composition and experimental conditions, it may be concluded that Cu/Zn/Al catalysts obtained from hydrotalcite-like precursors compare favorably, in terms of high $H_2$ yield and low CO production, with those obtained by impregnation or hydroxide precipitation. It is likely that catalytic properties are improved by the method of homogeneous precipitation employed for preparation of the precursor, because this method leads to higher surface areas and more homogeneous materials, as suggested by the previous XRPD and TPR characterization of these systems [31]. A recent paper [36] dealing with the SRM reaction has evidenced better catalytic performances of Cu/Zn/Al catalysts prepared by the method of urea hydrolysis in comparison with similar catalysts obtained by the coprecipitation method.

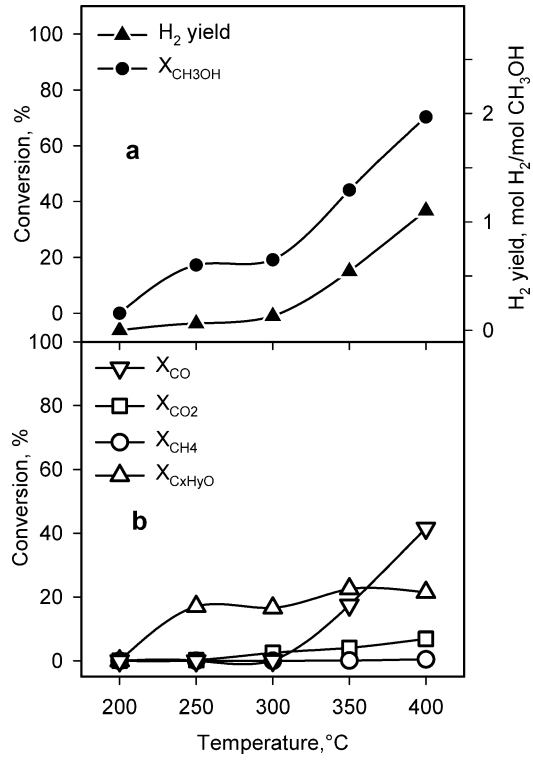


Fig. 6. (a) Methanol conversion and hydrogen yield; (b) conversions to different products as a function of temperature under DEC conditions for the catalyst 10-Cu/Zn/Al, GHSV $= 0.6 \times 10^5\ h^{-1}$.

For a better understanding of the reaction path, tests of simple steam reforming (SRM), decomposition (DEC), and partial oxidation (POM) of methanol are carried out on the catalyst 10-Cu/Al/Zn at GHSV $= 0.6 \times 10^5\ h^{-1}$ and the results are plotted in Figs. 5–7. As expected, in SRM tests (Fig. 5) lower conversions of methanol than under OSRM conditions are found at all temperatures; $CO_2$ and $H_2$ are selectively produced due to very limited formation of methane and $C_xH_yO$ that are produced in some amount only at 250 °C. The concentrations of CO are below the detection limit also under these conditions. In DEC tests (Fig. 6) the catalyst appears less active than in SRM tests. The decomposition products, $H_2$ and CO, are formed in appreciable amounts only at $T > 300$ °C. The maximum $H_2$ yield, attained at 400 °C, is about 1, which is lower than that expected from methanol conversion, taking into account the decomposition stoichiometry. This is explained by the occurrence of side reactions. In fact, besides CO and $H_2$, also $C_xH_yO$, $CO_2$, and traces of $CH_4$ are produced. $C_xH_yO$ are the only reaction products at $T \leqslant 300$ °C, while small amounts of $CO_2$ are formed at high temperatures. The catalyst is tested also for POM reaction, and the results are shown in Fig. 7. The production of $CO_2$ and $H_2$ starts at 300 °C, while at lower temperatures $C_xH_yO$ are the only reaction products. $CO_2$ and $H_2$ are formed at 300 °C in amounts corresponding to complete $O_2$ consumption and stoichiometry of Eq. (2). By increasing temperature $H_2$ yield increases up to 1.6 mol $mol^{-1}$ at 400 °C: at the same time

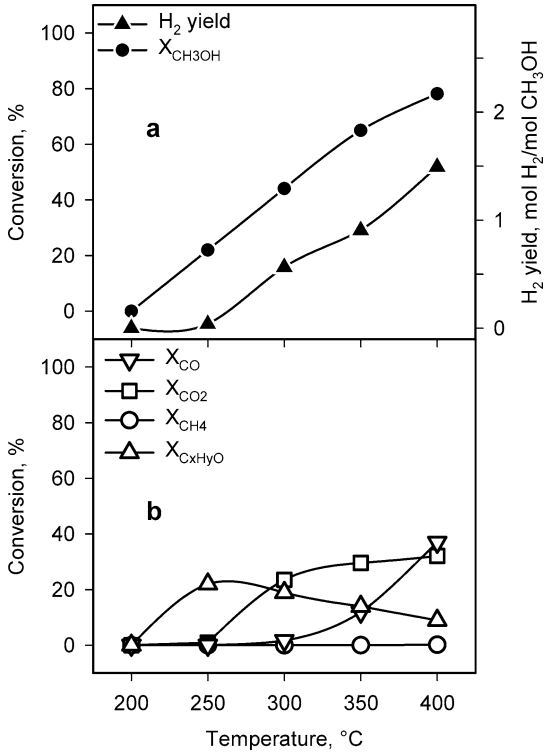


Fig. 7. (a) Methanol conversion and hydrogen yield; (b) conversions to different products as a function of temperature under POM conditions for the catalyst 10-Cu/Zn/Al, GHSV $= 0.6 \times 10^5\ \mathrm{h}^{-1}$.

conversion to CO increases, while conversion to $CO_2$ is almost constant in the range 300–400 °C. This suggests that at $T > 300$ °C reaction (2) is complete and residual methanol undergoes decomposition into CO and $H_2$.

From these results we can observe that SRM is faster than decomposition, being activated at lower temperature (Figs. 5 and 6) and POM is faster than SRM, since at 300 °C conversion to $CO_2$ is higher in POM than in SRM tests (Figs. 5 and 7), although the low $O_2$ partial pressure limits the extent of the reaction. The products $C_xH_yO$ prevail at low temperatures, suggesting faster dehydrogenation and dehydration reactions. Therefore it can be supposed that the activation energies of SRM, POM, methanol decomposition (DEC), dehydration (DEHD), and dehydrogenation (DEHG) increase in the following order:

DEHD, DEHG < POM < SRM < DEC.

At low temperatures (200–250 °C) the kinetics of SRM and POM is low and only dehydration and dehydrogenation occur to some extent. By increasing temperature, first POM and after SRM reactions are activated. POM can go forward to a small extent due to the limited concentration of $O_2$, and then residual methanol reacts through SRM or DEC.

### 3.2. The reaction network

The above data show that OSRM involves a complex network of parallel and series reactions.

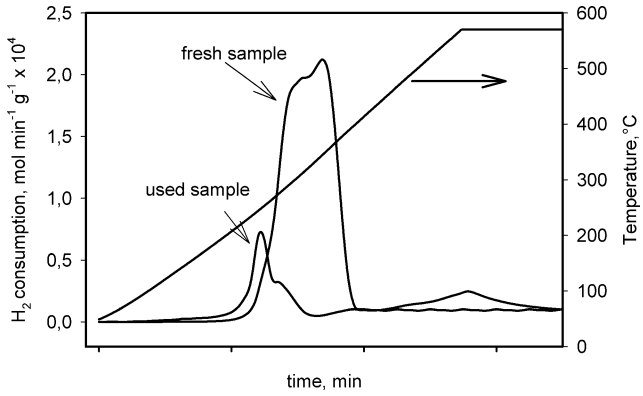


Fig. 8. TPR profile of fresh (oxidized) and used 10-Cu/Zn/Al sample.

Methanol total oxidation,

$$CH_3OH + \frac{3}{2}O_2 = CO_2 + 2H_2O, \qquad (5)$$

can occur on CuO-based catalysts [37]. It is hypothesized that in OSRM with Cu catalysts methanol combustion occurs rapidly, so oxygen is consumed in the first region of the reactor, and the SRM reaction begins when oxygen has been consumed [24,28]. Previous TPR/TPO measurements [31] suggest that under OSRM conditions Cu(0), Cu(I), and Cu(II) species can be present, depending on temperature and $O_2$ and $H_2$ concentrations. Therefore in the zone where $O_2$ concentration is high, copper is in an oxidized state, and methanol oxidation prevails. On the other hand, in the zone where $O_2$ is low and $H_2$ concentration is high, copper is in a reduced form and steam reforming becomes the dominant reaction. Reaction (5) is not a parasitic reaction because, if it is followed by reaction of produced $H_2O$ with $CH_3OH$, the net result is POM reaction, as already observed [1,22].

With the aim to investigate the Cu oxidation state of the catalysts under OSRM conditions, TPR measurements have been carried out on the samples after OSRM tests. In Fig. 8 the TPR profile of the sample 2-Cu/Zn/Al is reported together with that of the oxidized sample, for comparison. It can be observed that the spectrum of the used sample shows a low intensity signal at 240 °C. This signal contains different components that cannot be explained only by stepwise reduction of some Cu(II) to Cu(0), but are probably related to the presence of copper species with different oxidation states. The total $H_2$ consumption is 0.2 mol $\mathrm{mol}^{-1}$, which corresponds to a mean Cu oxidation state of 0.4, as if 20% of Cu were oxidized to Cu(II) (but probably Cu(I) and Cu(II) are present together). This indicates that under OSRM conditions copper is present in both oxidized and reduced states, but the Cu(0) state prevails. These data seem to confirm that there is a zone of the catalytic bed in which the catalyst is oxidized, and another zone in which it is reduced, and the latter zone is larger. This agrees with the faster kinetics of the oxidation reactions compared to that of steam reforming. Moreover it is worth noting that the TPR peak of the used samples appears at lower temperatures and with a shape different from that of the fresh calcined sample, showing that

Cu(II) species formed by oxidation of Cu(0) have properties different from those present in the original oxidized sample. A similar effect due to the reduction–reoxidation cycle was already observed for $CuO/ZnO/Al_2O_3$ catalysts and can be attributed to a structural modification that improves copper dispersion [24]. However the precise mechanism of such modification is not clear.

As observed in the Section 1, the steam reforming reaction (3) is formally the sum of methanol decomposition (1) and water gas shift (2): it is debated if SRM really occurs through the sequence of reactions (1) and (2) [34,38] or is a single reaction [1,7,8]. It is well known that both reactions (1) and (2) can be catalyzed by copper-based catalysts [7,39]; however, if this sequence were the main pathway for SRM, on the basis of equilibrium calculation, the expected CO concentration would be about 1% at 200 °C and 5% at 400 °C under our experimental conditions. Since all OSRM and SRM tests produced CO concentrations well below these values, we conclude that the sequence of reactions (1) and (2) is not the main pathway for SRM reaction, and this is probably a single reaction, in agreement with other studies [1,7,8].

An other open question is the pathway for CO formation. As above observed, CO is formed in appreciable amounts in POM and DEC tests at $T > 300$ °C. It is evident that in DEC tests CO is formed by methanol decomposition (1), possibly through intermediate dehydrogenation to formaldehyde (6),

$$CH_3OH = CH_2O + H_2, \tag{6}$$

and probably the same reaction(s) occur in POM tests.

On the other hand, in SRM and OSRM tests the formation of CO is reduced below the detection limit: this behavior can be attributed to the presence of water vapor. A decrease of CO production from methanol due to the presence of water vapor is reported in recent works on Cu catalysts [24,40] and this effect is explained by the WGS reaction (2) consuming CO [40]. However, as observed above, the WGS reaction is unable to reduce the CO concentration to very low values as found in our SRM and OSRM tests. As a possible explanation, we hypothesize that the presence of water vapor shifts the methanol reaction toward $CO_2$ rather than CO by modifying the catalyst properties, that is causing some oxidation of Cu, as discussed in the following (see reaction mechanism).

According to some authors [1,24,32] CO can be produced under SRM or OSRM conditions by the reverse of the WGS reaction (2). It is obvious that this reaction is very limited under the present conditions. Probably this reaction is slower than SRM, as also suggested by [1,41].

The formation of methane as by-product of OSRM was not considered in previous works. Methane can be formed by the reaction (7)

$$CO + 3H_2 = CH_4 + H_2O \tag{7}$$

that is highly favored in the whole temperature range. The activity of CuO/ZnO-based catalysts for CO methanation has been reported [42]. This reaction can contribute to keep the CO concentration at a low level. Methane is formed in appreciable amounts in OSRM tests at high temperatures (Figs. 1–4), while it is negligible in DEC and POM tests, although CO production is high under these conditions. This is probably due to the low $H_2$ concentrations that reduce the kinetics of methanation. Also under SRM conditions methane is negligible, probably due to very low CO production, as observed above. The formation of appreciable amounts of $CH_4$ in OSRM tests can be explained by the higher methanol conversions, in comparison with SRM tests. This leads to lower $H_2O$ concentrations: under these conditions the unfavorable effect of steam on CO production is reduced, so that appreciable CO amount can be formed. This is readily converted into $CH_4$, due to the high $H_2$ concentration.

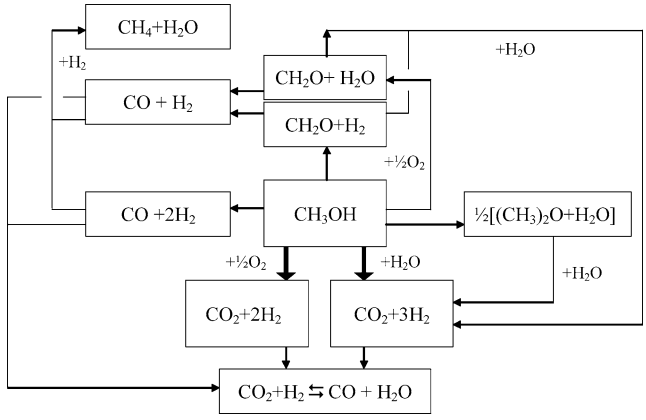


Fig. 9. Reaction network under OSRM conditions.

On the basis of the above discussion, the following network for OSRM can be proposed (Fig. 9). The scheme also includes methanol condensation to dimethylether that occurs probably on acid sites of $Al_2O_3$, being a well-known acid-catalyzed reaction, and oxidative dehydrogenation to formaldehyde (8), which is known to occur on Cu-based catalysts [43]:

$$CH_3OH + \frac{1}{2}O_2 = CH_2O + H_2O. \tag{8}$$

Reaction (8) could explain the results obtained in OSRM tests at low temperatures, that is, some methanol conversion with no $H_2$ or $CO_2$ production (Figs. 2 and 4). Moreover reactions consuming $CH_2O$ and $(CH_3)_2O$ are also taken into account. In fact the maxima observed in the curves of conversion to $C_xH_yO$ (Figs. 1–4) may be due to reactions consuming these products, that prevail at high temperature. These can be steam reforming reactions (9) and (10):

$$CH_2O + H_2O = CO_2 + 2H_2, \tag{9}$$

$$(CH_3)_2O + 3H_2O = 2CO_2 + 6H_2. \tag{10}$$

Reaction (9) can occur on Cu-based catalysts, as suggested by mechanistic studies [32]. Reaction (10) is also reported for Cu-based catalysts [44].

Obviously, the scheme in Fig. 9 does not include oxidation reactions, that can involve all combustible species:

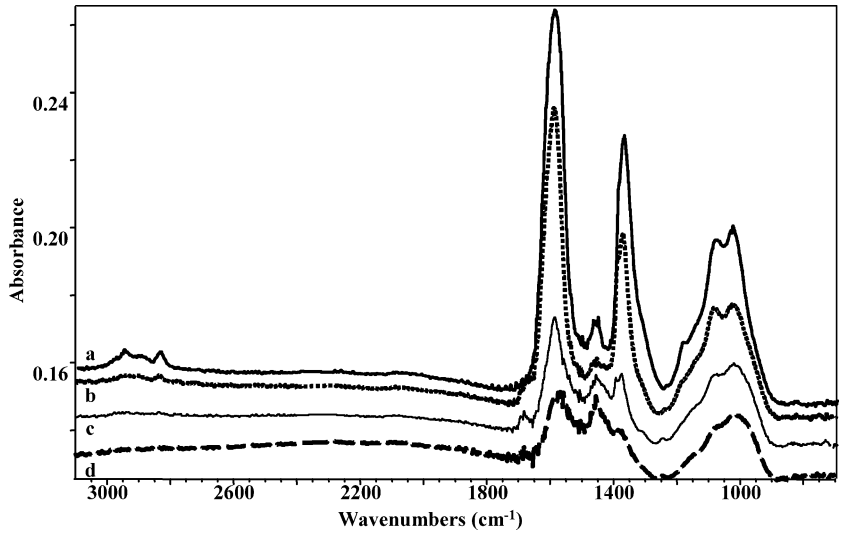


Fig. 10. FTIR subtraction spectra; the spectrum of the 10-Cu/Zn/Al catalyst after reduction was subtracted from the spectra of pure powder: (a) surface species after contact of the catalyst with $CH_3OH$ at 250 °C for 10 min; (b) surface evolution after 10 min at 300 °C; (c) surface evolution after 10 min at 350 °C; (d) surface evolution after 10 min at 400 °C.

$CH_3OH$, $CH_2O$, $(CH_3)_2O$, $H_2$, CO, $CH_4$. These reactions are limited by the defective $O_2$ amount and can occur only in the reactor zone where $O_2$ is still present.

Eventual reactions producing carbonaceous compounds, such as polymerization or condensations, can be excluded since the elemental analysis of the catalysts used in the tests has shown the absence of carbon compounds.

### *3.3. FTIR study of methanol adsorption and reaction mechanism*

The IR spectrum of the adsorbed species arising from the interaction of methanol at 250 °C with the prereduced catalyst (10-Cu/Zn/Al sample) is shown in Fig. 10a. In the low-frequency side of the spectrum a complex band with two main maxima at 1031 and 1088 $cm^{-1}$ is observed. However, a well-defined component is observed, weak, at 1191 $cm^{-1}$, while other components are envisaged near 1120 and 950 $cm^{-1}$. In the CH stretching region weak bands with two sharp maxima at 2953 and 2839 $cm^{-1}$ and a weaker broad maximum in the middle (2889 $cm^{-1}$) are also found, corresponding to a sharp $CH_3$ deformation band at 1469 $cm^{-1}$. These features can be assigned to adsorbed methoxy groups. The multiplicity of the band in the region 1200–900 $cm^{-1}$ is due very likely to the presence of two or more kinds of methoxy groups. As for comparison, we can note that the C–O stretching of methoxy groups on $\gamma$-$Al_2O_3$ is found at 1095 $cm^{-1}$ [45], and those on ZnO- and ZnO-based systems [46] at 1060 $cm^{-1}$. Those on CuO are reported to be very labile, whose C–O stretching is found at 1055–1070 $cm^{-1}$, and finally, those on Cu(111) [47] at 1036 $cm^{-1}$. The sharper component at 1191 is most likely due to the rocking $CH_3$ mode of the same methoxy groups.

However, already at low temperatures we can find sharp strong bands at 1598, 1381 (shoulder), and 1376 $cm^{-1}$. This spectrum is typical of formate ions [45] and have to be assigned to asymmetric stretching of the O–C–O group (1598 $cm^{-1}$), the CH deformation mode (1381 $cm^{-1}$), and, finally, to the symmetric O–C–O stretching (1376 $cm^{-1}$).

Under the same conditions of Fig. 10a, the gas phase species evolved from the catalyst have been also studied. The spectrum of the gas in contact with the catalyst at 250 °C is dominated by the features of gaseous methanol, although the features of gaseous water are clearly also present. Actually, a very weak band at 2140 $cm^{-1}$ due to gaseous CO and two weak features near 1178 and 1103 $cm^{-1}$, likely belonging to dimethylether gas, can also be detected.

By increasing temperature in the IR cell, the spectra of adsorbed species change as reported in Figs. 10b–d. It is evident that the spectra of both methoxy groups and formate groups decrease progressively in intensity. However, while the bands of formate groups are practically fully disappeared at 400 °C, the main band of methoxy groups at 1100–900 $cm^{-1}$ is still present, although much weaker and with the main maximum shifted down to 1016 $cm^{-1}$. In parallel the band now observed near 1458 $cm^{-1}$ seems to have grown, likely due to the formation of carbonate species. After heat treatment at 300 and 350 °C a weak sharp band at 1690 $cm^{-1}$ is evident. It can be assigned to the C=O stretching of an adsorbed formaldehyde species [45]. The presence of dioxymethylene species, a likely intermediate in the conversion to methoxy groups into formates, cannot be excluded, due to the presence of weak additional components at 1245 $cm^{-1}$ and in the range 1180–1090 $cm^{-1}$ [48].

Looking at the gas evolving from the surface (Fig. 11), only very small amounts of methanol are desorbed at 300 °C, CO being mostly produced up to 400 °C. As it is well known, hydrogen gas is IR undetectable.

The IR spectra reported above show that the adsorption of methanol on the catalyst is dissociative. Methoxy groups

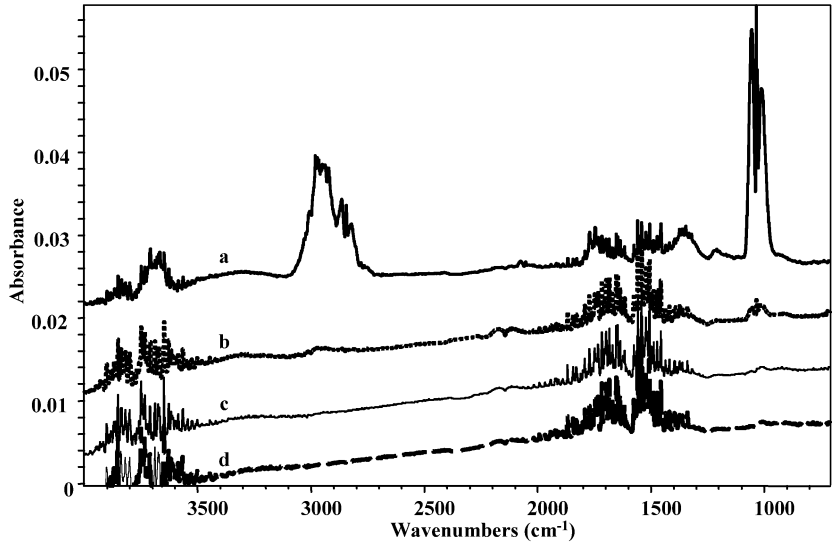


Fig. 11. FTIR spectra of the gas phases evolved after 10 min at (a) 250 °C; (b) 300 °C; (c) 350 °C; (d) 400 °C.

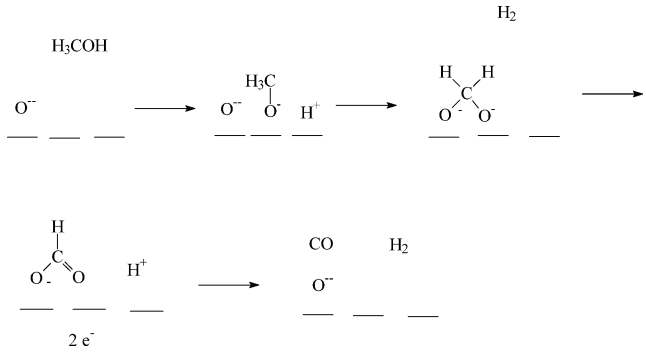


Fig. 12. Reaction mechanism of $CH_3OH$ decomposition.

are formed that apparently adsorb both on the active sites (which are likely associated to Cu species) and over inert regions of the catalyst surface, likely mainly associated to alumina. Part of these methoxy groups, likely those located near or on copper sites, transform easily to formate species, possibly with the intermediacy of dioxymethylene species. Traces of formaldehyde adsorbed as such are also detectable. At 300 °C or above formate species decompose and, under the conditions of our experiment, mainly give rise to gas-phase CO. Dimethylether is also found in the gas phase. The mechanism of methanol decomposition, consequently, is reasonably proposed as formed by the reaction scheme of Fig. 12, as proposed previously [46].

It seems quite reasonable to suppose that the mechanisms for DEC, POM, and SRM are closely related, and that the surface phenomena are similar. However, the flow catalytic data give some interesting information. In particular, the conversion of methanol in the presence of both water (SRM) and oxygen (POM) is higher than under the conditions of DEC. This could be due to an effect of these substances on the oxidation state of Cu. Moreover, CO is produced in relative low amounts in the presence of water (SRM conditions), $CO_2$ being the largely predominant product. On the other hand, both CO and $CO_2$ are produced in noticeable amounts under POM conditions. To explain this we can resume the data concerning CO adsorption on Cu species, as determined by IR spectroscopy. Previous data [31] show that CO is adsorbed very weakly on Cu metal particles, while it is adsorbed very strongly on Cu(I) centers. On the other hand, Cu(II) easily oxidizes CO to $CO_2$. It seems quite likely that upon DEC experiments, the catalyst is fully reduced. Under these conditions CO is formed by formate species decomposition and is easily desorbed as the product. On the contrary, under the conditions of POM the catalyst is, at least partially, oxidized. In this case Cu(I) strongly adsorbs CO while Cu(II) allows its oxidation to $CO_2$ before its desorption. The true product of POM is consequently $CO_2$. However, due to the substoichiometric feed in POM tests, it can be supposed that oxygen is consumed in the upper reactor zone, so the catalyst in the lower zone is reduced. This means that after $O_2$ is consumed, excess methanol decomposes (partially) producing CO. A somewhat different behavior is observed under SRM conditions, since CO production is negligible in this case. We can suppose that the presence of excess water vapor oxidizes the catalyst, at least partially, leading to formation of Cu(II) species that produce $CO_2$ at the expense of CO. Such oxidation should be only partial, according to TPR measurements on the used catalysts that show a low mean oxidation state of Cu, as seen above.

## 4. Conclusions

Cu–Zn–Al catalysts derived from a hydrotalcite-like precursor have been studied for oxidative reforming of $CH_3OH$. Good results, in terms of $CH_3OH$ conversion and $H_2$ yield, together with low CO production, have been obtained, showing that the method of homogeneous precipitation of hydrotalcite-like precursors is suitable for preparing high

activity catalysts. Methanol decomposition appears a reaction slower than steam reforming and partial oxidation and is greatly depressed by water vapor. A noticeable catalytic activity for methanation has been evidenced in high temperature tests: this property appears unfavorable for hydrogen yield, but could be advantageous for developing catalysts with very low CO selectivity.

The reaction network involves also dehydrogenation to formaldehyde and dehydration to dimethylether, the WGS reaction, besides oxidation reactions.

The reaction mechanism has been studied by IR technique, that evidenced different species formed by adsorption of methanol on the catalyst. The hypothesized mechanism points to an important role of Cu(I) and Cu(II) species: Cu(I) strongly adsorbs CO, while Cu(II) catalyzes CO oxidation to $CO_2$. The oxidation state of Cu species is influenced by the presence of $O_2$ and $H_2O$.

Work is in due course in our Laboratories to study the effect of the preparation methods of the Cu–Zn–Al precursors on the selectivity and activity of the OSRM catalysts thereby obtained.

## Acknowledgments

This research was founded by Ministero Istruzione Università e Ricerca and Genova, Napoli and Perugia Universities, in the framework of Programmi di Ricerca di Interesse Nazionale, 2002 No. 038793. The authors acknowledge Mr. Luciano Cortese for his contribution to catalytic activity tests.

## References

[1] K. Geissler, E. Newson, F. Vogel, T.B. Truong, P. Hottinger, A. Wokaun, Phys. Chem. Chem. Phys. 3 (2001) 289.
[2] X. Liu, O. Korotkikh, R. Farrauto, Appl. Catal. A 226 (2002) 293.
[3] P.J. de Wild, M.J.F.M. Verhaak, Catal. Today 60 (2000) 3.
[4] D.J. Moon, K. Sreekumar, S.D. Lee, B.G. Lee, H.S. Kim, Appl. Catal. A 215 (2001) 1.
[5] B. Lindström, L.J. Pettersson, J. Power Sources 118 (2003) 71.
[6] R.O. Idem, N.N. Bakhshi, Chem. Eng. Sci. 51 (1996) 3697.
[7] J.P. Breen, J.R.H. Ross, Catal. Today 51 (1999) 521.
[8] B.A. Peppley, J.C. Amphlett, L.M. Kearns, R.F. Mann, Appl. Catal. A 179 (1999) 21.
[9] L. Ma, B. Gong, T. Tran, M.S. Wainwright, Catal. Today 63 (2000) 499.
[10] Y.M. Lin, M.H. Rei, Catal. Today 67 (2001) 77.
[11] A.P. Tsai, M. Yoshimura, Appl. Catal. A 214 (2001) 237.
[12] T. Takahashi, M. Inoue, T. Kai, Appl. Catal. A 218 (2001) 189.
[13] M.M. Günter, T. Ressler, R.E. Jentoft, B. Bems, J. Catal. 203 (2001) 133.
[14] Y. Liu, T. Hayakawa, K. Suzuki, S. Hamakawa, T. Tsunoda, T. Ishii, M. Kumagai, Appl. Catal. A 223 (2002) 137.
[15] Y.H. Chin, R. Dagle, J. Hu, A.C. Dohnalkova, Y. Wang, Catal. Today 77 (2002) 79.
[16] M.L. Cubeiro, J.L.G. Fierro, J. Catal. 179 (1998) 150.
[17] J. Agrell, K. Hasselbo, K. Jansson, S.G. Järas, M. Boutonnet, Appl. Catal. A 211 (2001) 239.
[18] Z. Wang, W. Wang, G. Lu, Int. J. Hydrogen Energy 28 (2002) 151.
[19] R.M. Navarro, M.A. Pena, J.L.G. Fierro, J. Catal. 212 (2002) 112.
[20] Z. Wang, W. Wang, G. Lu, J. Mol. Catal. A: Chem. 191 (2003) 123.
[21] J. Agrell, G. Germani, S.G. Jaras, M. Boutonnet, Appl. Catal. A 242 (2003) 233.
[22] J. Agrell, M. Boutonnet, J.L.G. Fierro, Appl. Catal. A 253 (2003) 213.
[23] B. Lindström, L.J. Pettersson, P.G. Menon, Appl. Catal. A 234 (2002) 111.
[24] J. Agrell, H. Birgersson, M. Boutonnet, I. Melián-Cabrera, R.M. Navarro, J.L.G. Fierro, J. Catal. 219 (2003) 389.
[25] S.H. Chan, H.M. Wang, J. Power Sources 126 (2004) 8.
[26] S. Murcia-Mascarós, R.M. Navarro, L. Gómez-Sainero, U. Costantino, M. Nocchetti, J.L.G. Fierro, J. Catal. 198 (2001) 338.
[27] S. Velu, K. Suzuki, M.P. Kapoor, F. Ohashi, T. Osaki, Appl. Catal. A 213 (2001) 47.
[28] T.L. Reitz, P.L. Lee, K.F. Czaplewski, J.C. Lang, K.E. Popp, H.H. Kung, J. Catal. 199 (2001) 193.
[29] J.-P. Shen, C. Song, Catal. Today 77 (2002) 89.
[30] S. Liu, K. Takahashi, M. Ayabe, Catal. Today 87 (2003) 247.
[31] M. Turco, G. Bagnasco, U. Costantino, F. Marmottini, T. Montanari, G. Ramis, G. Busca, J. Catal. 228 (2004) 43.
[32] J.P. Breen, F.C. Meunier, J.R.H. Ross, Chem. Commun. (1999) 2247.
[33] F. Raimondi, K. Geissler, J. Wambach, A. Wokaun, Appl. Surf. Sci. 189 (2002) 59.
[34] S. Velu, K. Suzuki, M. Okazaki, M.P. Kapoor, T. Osaki, F. Ohashi, J. Catal. 194 (2000) 373.
[35] I.A. Fisher, A.T. Bell, J. Catal. 184 (1999) 357.
[36] T. Shishido, Y. Yamamoto, H. Morioka, K. Takaki, K. Takehira, Appl. Catal. A 263 (2004) 249.
[37] T.L. Reitz, S. Ahmed, M. Krumpelt, R. Kumar, H.H. Kung, J. Mol. Catal. A: Chem. 162 (2000) 275.
[38] J.C. Amphlett, M.J. Evans, R.F. Mann, R.D. Weir, Can. J. Chem. Eng. 66 (1988) 950.
[39] B.A. Peppley, J.C. Amphlett, L.M. Kearns, R.F. Mann, Appl. Catal. A 179 (1999) 31.
[40] Y. Choi, H.G. Stenger, Appl. Catal. B 38 (2002) 259.
[41] H. Purnama, T. Ressler, R.E. Jentoft, H. Soerijanto, R. Schlögl, R. Schomäcker, Appl. Catal. A 259 (2004) 83.
[42] V.I. Sharkina, G.I. Salomatin, N.N. Aksenov, V.S. Sobolevskii, Kinet. Katal. 25 (1984) 765.
[43] C.N. Satterfield, Heterogeneous Catalysis in Practice, McGraw-Hill, New York, 1980, p. 195.
[44] K. Nakamura. Y. Hiramatsu, JP 2003038957 (2003), to Mitsubishi Gas Chemical Co., Ltd., CAN: 138:156226.
[45] G. Busca, P.F. Rossi, V. Lorenzelli, M. Benaissa, J. Travert, J.C. Lavalley, J. Phys. Chem. 89 (1985) 5433.
[46] A. Riva, F. Trifirò, A. Vaccari, L. Mintchev, G. Busca, J. Chem. Soc., Faraday Trans. 1 84 (1988) 1423.
[47] M.A. Chester, E.M. McCash, Spectrochim. Acta A 43 (1987) 1625.
[48] G. Busca, J. Lamotte, J.C. Lavalley, V. Lorenzelli, J. Am. Chem. Soc. 109 (1987) 5197.